RESEARCH ARTICLE	OPEN ACCESS

Prediction of Radio Refractivity from Meteorological Parameters in Tropical Region Using a Modified Artificial Neural Network

Aremu, OlaosebikanAkanni[(1*)]**., Olabisi, Olusegun**[(2)]**,Sheu, Akeem Lawal**[(3)]

Amodu, FunkeRoseline[(4)]

[(1*)] Department of Physics, The Polytechnic, Ibadan.Nigeria
[(2)] Department of Science Laboratory Technology, LadokeAkintola University of Technology, Nigeria and   Department of Physics, Ajayi Crowther university, Oyo, Nigeria.
[(3)]Department of Physics, Emmanuel Alayande College of Education. P.M.B. 1010, Oyo. Nigeria
[(4)]Department of Physics, Federal Polytechnic, Ede. Osun State, Nigeira.

Corresponding author: oolabisi@lautech.edu.ng

Abstract - Atmospheric radio refractivity variation in troposphere is one of the parameters that influence electromagnetic wave propagation and its effect at the troposphere is very important in system planning for communication links. In this study, a machine learning/artificial neural network (ANN) based model is applied to predict the radio refractivity. High resolution Radiosonde meteorological data (air temperature, atmospheric pressure and relative humidity) obtained from the Nigerian Meteorological agency, NiMet, Ibadan, South Western Nigeria (7° 22'39''N, 3° 54' 21''E) were used as ANN inputs. ITU-R models was used in obtaining radio refractivity, N, which served as target for the ANN. The inputs and target values were trained based on the Levenberg–Marquardt algorithm, the mean square error for Tan-Sigmoid (tansig) and Pureline transfer functions were used in the hidden and output layers respectively, and 3-5-1 topology provided the best results. The generated weights and bias values of the best performed SLN were extracted for the development of the ANN based Refractivity model. The results revealed that, the refractivity values are higher during the rainy season owing to a strong association with the temperature and relative humidity. The minimum average radio refractivity value (365.2 N-units) was obtained in the month of February (dry season) while higher value of 383 N-units was obtained for the month of September (rainy season). Therefore, it is important to properly cater for the communication system (signal) during hot and humid weather. Furthermore, the developed model has an acceptable accuracy value as demonstrated from comparison of results with actual measured values with lowest mean square error. Based on the results, the proposed ANN method can be used to develop a refractivity database which is highly important in a radio communication system.

Key words: ANN, Levenberg–Marquardt, meteorological parameters, Refractivity, Troposphere

1. INTRODUCTION

Propagation of Radio signal are affected by the nature of the atmosphere and the signal can be scattered, absorbed, reflected, or refracted due to numerous atmospheric behaviors (Adeniran, et.al, 2020) . The basic factors that affect the radio links, frequency and signal strength in the troposphere are: pressure, temperature, and relative humidity which are primary weather parameters (Gao, *et.al.,* 2008). The effects of the factors aforementioned leads to variation in the refractive index of the Troposphere andthe primary weather parameters also affects the refractivity gradient as well as the effective earth radios factor as reported by (Aremu, et.al., 2021). Also, multipath effects arise due to large scale variations in atmospheric radio refractive index, such as horizontal layers with very different refractivity (Grabner and Kvicera, 2003). This effect becomes manifest, when the same signal takes different paths to its target and the rays arriving at different times thereby interfering with each other during propagation through the troposphere. The effects of this large scale variation in the tropospheric refractive index is that radio waves propagating through the atmosphere become progressively curved towards the earth while small variations in these parameters can bring about a substantial effect on the propagation of radio waves, which is due to the fact that the radio signals are refracted over a complete signal path which often degrade communication links (Falodun and Ajewole 2006), (Valma, et.al., 2015) In this study, the atmospheric pressure, temperature and water vapor pressure of the air was measured and indirect method was utilized to determine the radio tropospheric refractivity using empirical formula provided by International Telecommunication Union. The study further illustrates the applications of the feed forward back propagation with hyperbolic tangent neurons in the hidden layer and linear neuron in the output layer of ANN to predict the monthly radio refractivity in Ibadan, south western Nigeria

2. THEORETICAL BACKGROUND

The radio refractive index is defined as the ratio of the speed of propagation of radio energy in a vacuum to the speed in a specified medium as shown in Equation (1)

$$n = \frac{C_v}{C_m} \quad (1)$$

The refractive index of air, *n*, is measured by refractivity, N, and the two parameters are related as (Babin, 1995)

$$N = (n-1) \times 10^6 \quad (2)$$

The radio refractive index may be measured directly if the measuring instrument is sensitive to the speed of propagation. It is measured indirectly by measuring temperature, pressure, and humidity with subsequent conversion to the refractive index as shown below;

The radio refractivity is derived in terms of the primary weather parameters(Temperature, water vapour pressure and atmospheric pressure) using equation(6)

$$N_{(T,P,e)} = N_{dry} + N_{wet} \quad (3)$$

where

$$N_{dry} = \frac{77.6P}{T} \quad (4)$$

$$N_{wet} = 3.732 \times 10^5 \frac{e}{T^2} \quad (5)$$

$$N_{(T,P,e)} = \frac{77.6P}{T} + 3.732 \times 10^5 \frac{e}{T^2} \quad (6)$$

Equation (6) is used to determine radio refractivity up to the frequencies of 100 GHz with error less than 0.5%. (Bean and Thayer, 1959). The water vapour pressure, e, is quantified using Equation (7)

$$e = \frac{RH}{100} \, a \exp\left(\frac{bt}{t+c}\right) \quad (7)$$

where *RH* represents the relative humidity, *t* is the temperature (°C). Moreover, the coefficients are given as: $a = 6.1121$, $b = 17.502$, and $c = 240.97$. These coefficients are valid from −20 to 50 °C with an accuracy level $\pm 0.2\%$(Tohidi, 2012), (ITU – R., 2012).

3. METHODOLOGY

Indirect method of measuring radio refractivity was employed to determine the radio refractivity. The meteorological data used are high-resolution radiosonde data form the Nigerian Meteorological agency, NiMeT, Ibadan, South Western Nigeria (7° 22'39''N, 3° 54' 21''E).The meteorological data obtained in the year 2021 includes: air temperature, relative humidity and atmospheric pressure at the height of the sounding balloon. Data collected from January to December 2021 were averaged over each hour to give twenty-four data point. The hourly data for each day is further averaged to give a data point for the day and average was taken over the month to give a data point for each month which was used to determine the monthly variations for the year. The obtained

meteorological data were used to compute the surface radio refractivity using Eq. (6). Nigeria latitude falls within the tropical zone but the climatic conditions are not totally tropical in nature, it varies in most parts of the country. In the north the climatic condition is very dry and it is equatorial in the south. The weather condition can be generally categorized into wet season (from April to October); dry season (from November to March).Fig.1 depicts the google map of the measurement campaign.

Fig.1 Map showing the study area (Google Maps, 2020).

3.1 TREATMENT OF DATA AND DEVELOPMENT OF ARTIFICIAL NEURAL NETWORK

A minimum-maximum normalization process was performed on the inputs and preprocessed Radio refractivity dataset obtained along the three itineraries using equation(9). This was done to prevent impulsive changes due to large variation in the datasets

$$y = \frac{(y_{max} - y_{min}) \times (x_{in} - x_{min})}{(x_{max} - x_{min})} + y_{min} \quad (8)$$

Since $y_{min} = -1$ and $y_{max} = +1$, x_R is the original data, y is the result of normalization. Equation (8) becomes,

$$y = \frac{2(x_{in} - x_{min})}{(x_{max} - x_{min})} - 1 \quad (9)$$

the normalized parameters were subjected to the ANN algorithm for training the data. For any configuration to be trained, the algorithm used randomly splits the data into 70% for training, 15% for Test, and 15% for Validation. In this study, a single-layered Levenberg-Marquardt with feed forward back propagation learning algorithm ANN architecture which encompassed four input neurons and one output neuron was designed for model training and

development, as shown in Figure 2. The ANN model design, training, validation, and testing were all done using a MATLAB 2020a produced by MathWorks Inc. Testing data-set comprised of data instances that are not included in the training data-set. The testing dataset was created to evaluate the generalization ability of the ANN models. The input data variables of the datasets include Temperature, relative humidity and atmospheric pressure. The single target output of the ANN model is the corresponding path loss values. The values of the input parameters are fed into the neurons in the input layer, while the output parameter (Radio refractivity) which depends on input parameters is the predicted variable. In ANN, the output layer accepts its input from the last hidden layer. Several configurations were trained before arriving at the best configuration for the modeling. Tansig transfer function was used at the hidden layer while purelin transfer function was used at the output layer as shown in equation(10)

$$y = \sum_{j=1}^{m} \left\{ Purelin \left[LW_{j,1} \left(\sum_{i=1}^{4} tansig(X_i IW_{i,j} + b_j) \right) \right] + b_o \right\} (10)$$

where Wij (or IW) represents the weights for input layer to hidden layer and LW represents hidden layer to output layer weights, b_j is the bias value for jth hidden neurons and b_o represents the bias for output neuron. During the training process, the epochs and goals were used as the stopping criteria to regulate the number of iterations and error tolerance respectively. The training stops once either the epoch or goal is reached. For this study, an epoch of 1,000 and a goal of zero were set.After denormalization and recovery phases, actual and forecasted testing datasets were evaluated. The network output with optimal configuration $3 \times 5 \times 1$ is obtained as follows:

$$E_{1,i,j} = \sum_{i=1\ldots2}^{j=1\ldots9} W1_{i,j}x_j * W1_{1,1}X_1 + W1_{1,2}X_2 + W1_{1,3}X_3 (11)$$

where , $W1_{1,1}$, $W1_{1,2}$, $W1_{1,3}$, refer to weights assigned to Temperature, relative humidity and atmospheric pressure respectively in the input (i) and for each neuron (j) in the hidden layer 1. The Tansig transfer function activates on $E_{1,i,j}$ to give $F_{1,i,j}$ defined as (12),

$$E_{1,i,j}(tansig) = F_{1,i,j} = \frac{2}{1 + \exp(-2E_{1,i,j})} - 1 \quad (12)$$

The weights and bias at the output layer transform $F_{1,i,j}$ to $O_{1,i,j}$ which is defined as:

$$O_{1,i,j} = \sum_{i=1}^{j} (WO_{ij} \times F_{ij}) + b_o (13)$$

where b_o and WO_{ij} are the bias at the weight at the output layer respectively. As depicts in figure 2, the transfer function (purelin) acts on equation(13) and transform it into the

normalized final output Radio refractivity (N) as shown in equation (14)

$$N = O_{1,i,j}(purelin) = \sum (WO_{ij} \times F_{ij}) + b_o (14)$$

The original value of the of the Radio refractivity output is obtained by denormalizing technique and it is simplified into

$$N = W_1F_1 + W_2F_2 + W_3F_3 + W_4F_4 + W_5F_5 + C \quad (15)$$

After denormalization and recovery phases, actual and forecasted testing datasets are evaluated. The performances of the trained data were examined for Radio refractivity forecasting in view of accuracy of predictions using the MSE which is given by:

$$MSE = \frac{1}{n} \sum_{i=1}^{n} (y_i - x_i)^2 (16)$$

where n is the number of sets in the output data. The weight and bias values are adjusted in order to obtain low MSE and thus increase the performance of the ANN. After this the training and retraining continues until the training data achieves the least MSE.

3.2 RELATIVE IMPORTANCE OF INPUT PARAMETERS ON ANN MODEL
In this study, the connection weights algorithm (Olden *et.al.,* 2004) which calculates the sum of products of final weights of the connections from input neurons to hidden neurons with the connections from hidden neurons to output neuron for all input neurons is used to determine the relative importance of the input parameters of the ANN model.

$$RI_X = \sum_{y=1}^{m} W_{xy}W_{yz} (17)$$

where RI_X is the relative impact of parameter x, W_{xy} is the final weights of the connection from input parameters to hidden neurons, W_{yz} the weights from the hidden neurons to output neuron, z is the output neuron 1 and y is the total number of hidden neurons which is 5.

4.   RESULTS AND DISCUSSION
4.1   RESULT OF TRANSFER FUNCTION
The effect of transfer functions at the hidden and the output layers during the machine learning is presented. In this process, the number of neurons in the hidden layer were kept constant while the transfer functions in the hidden layer were varied. Likewise, the transfer functions at the output layer were held constant. Subsequently, the number of neurons and the transfer function in the hidden layers were kept constant while the transfer functions at the output layer were varied. As depicts in Table 1. Best optimize networkthe network with least MSE (9.1×10^1) which is Tansig and Purelin at the hidden and output layers respectively which gave best accuracy than other sets was chosen

Table 1. Best optimize network

Hidden layer (HL)	Output layer	MSE	Variance
Tansig	Tansig	1.15×10^2	1.6×10^1
Tansig	**Purelin**	$\mathbf{9.1 \times 10^1}$	$\mathbf{1.9 \times 10^2}$
Tansig	Logsig	1.15×10^2	9.7×10^2
Logsig	Tansig	1.12×10^2	2.6×10^2
Logsig	Purelin	1.11×10^2	1.2×10^2
Logsig	Logsig	1.13×10^2	6.2×10^1
Purelin	Tansig	1.01×10^2	1.4×10^2
Purelin	Purelin	1.10×10^2	3.7×10^1
Purelin	Logsig	1.02×10^2	2.7×10^2

4.2 OPTIMAL CONFIGURATION

An ideal ANN configuration was obtained by varied the number of neurons in the hidden layer while the already transfer functions were held constant The results obtained in Table 2were used to determine the best among the configurations trained. The closer the value of NS to unity, the better the model derived from the configuration can predict the measured value. The optimal configuration with least AARE, NS, MSE and SSE but with higher correlation coefficient ($3 \times 5 \times 1$) was subsequently chosen. Hence, the choice of neuron number 5 was made as an ideal neuron in the hidden layer.Fig.2 shows the schematic diagram of the configuration while Fig.3 represents the configuration in the nodal form.

Table 2. Comparison of ANN configurations used in training.

ANN architectures	AARE	Nash-Sutcliffe coefficient. (NS)	MSE	SSE	Correlation. Coefficient. (R)
3-(3)-1	92	0.67	22	2123	0.8241
3-(4)-1	87	0.74	18	1740	0.8820
3-(5)-1	**48**	**0.92**	**13**	**1522**	**0.9548**
3-(6)-1	76	0.79	23	1815	0.7898
3-(7)-1	79	0.78	29	2105	0.7188
6-(8)-1	94	0.70	32	2263	0.7000
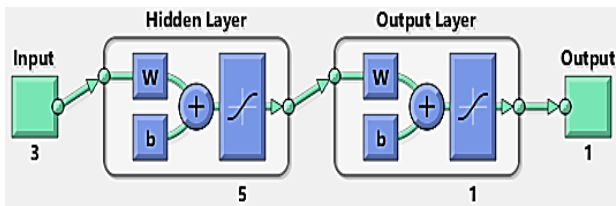
Fig.2 Schematic diagram of the $3 \times 5 \times 1$ ANN configuration
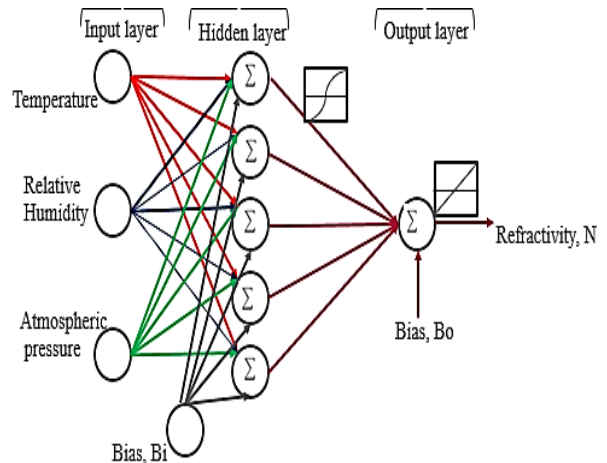

Fig.3A schematic ANN with 3-5-1 topology.

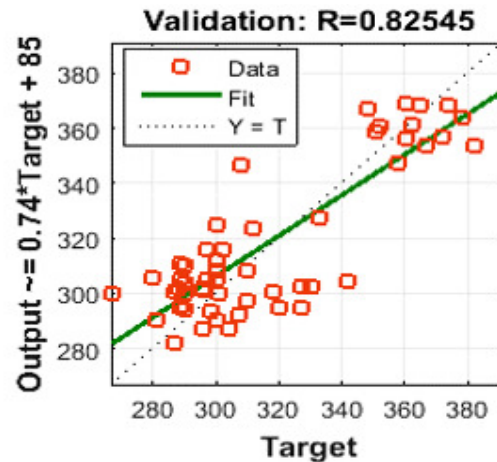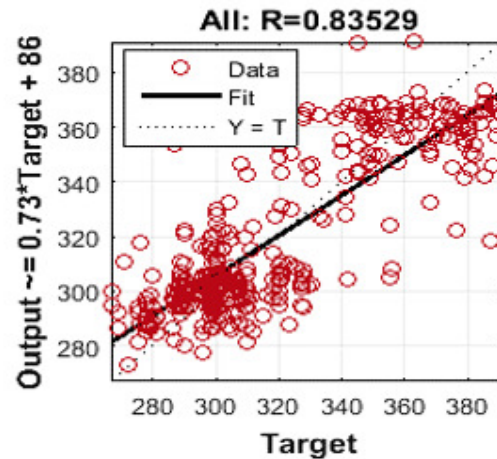### 4.3 PERFORMANCE OF THE ANN OPTIMAL CONFIGURATION

Fig. 4.3

Fig. 4.4

Fig.4.1 to 4.4 depicts the performance/degree of correlation of the network predicted radio refractivity values and their corresponding actual refractivity (target) for the training, testing and validation data.The best configuration which had minimum error and maximum regression coefficient was obtained with 5 neurons in the hidden layer. The network predicted model fits so well with the actual values for both training, testing and validation sets as gotten in their correlation coefficients (R) of 0.84096, 0.82973 and 0.82545 respectively while the R value for the overall of the model obtained is 0.83529. These values are higher than other configurations which indicate good accuracy in radio refractivity. It also provides a wide and rich class of reliable and powerful predictive tool to mimic complex nonlinear functional relationships for surface refractivity in this environment.
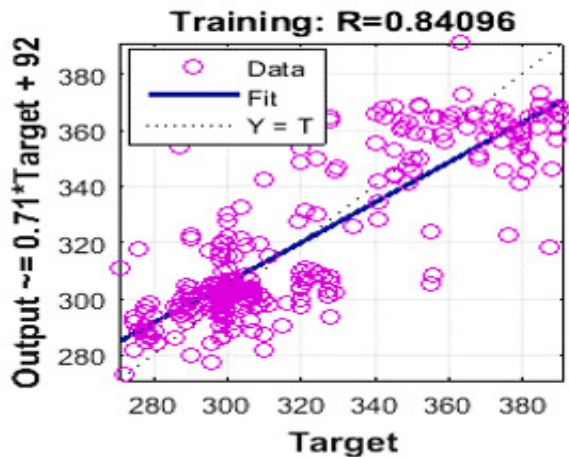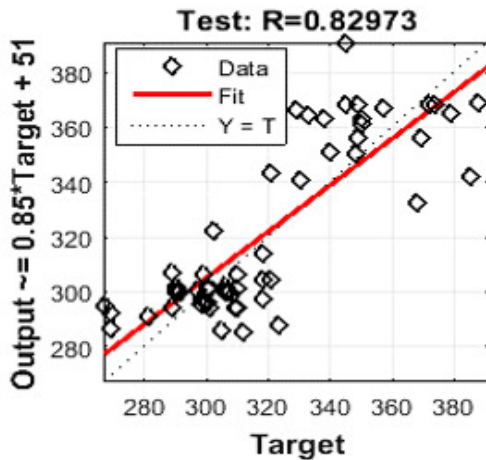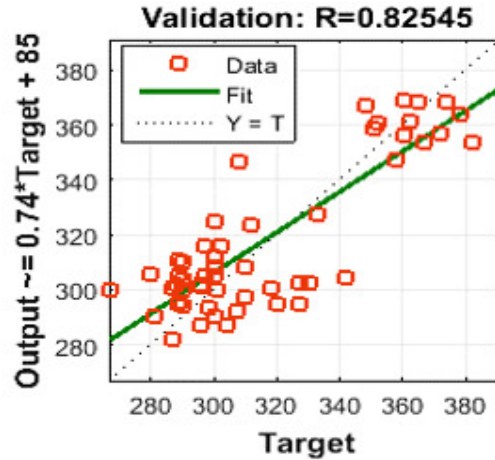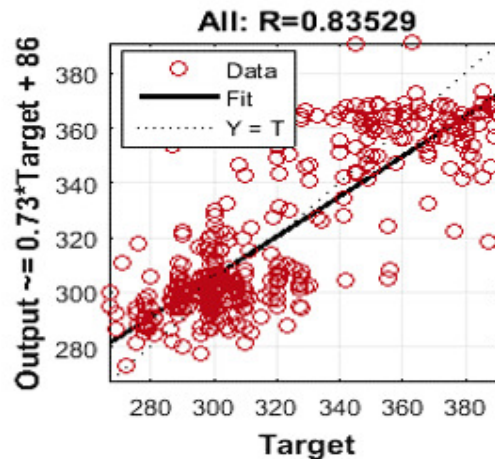

Fig. 4.3

Fig. 4.1

Fig. 4.4

Fig. 4.2

Fig.4.1 – 4.4: Training, Validation, Test and Overall performance of the training respectively for $3 \times 5 \times 1$ ANN

4.4 MODELING ANN RADIO REFRACTIVITY

The assigned weights and biases automatically generated during the training of the $3 \times 5 \times 1$ configuration were extracted and are as shown in Table 3

Table 3. Values of $E_{1,i,j}$ and $F_{1,i,j}$ obtained from ANN modeling of radio pathloss.

Weight to layer 1 from input 1			Bias to layer 1	Weight to layer 2. LW	Bias to layer 2
X1, j=1	X2, j=2	X3, j=3			
-7.113	-14.144	-3.856	33.9166	-8.5856	3.4558
12.396	5.675	-2.314	-3.6788	-0.25468	3.4558
-1.156	-1.451	0.013	-0.2071	-0.82116	3.4558
-18.355	12.472	-4.002	-6.9725	0.36799	3.4558
4.222	8.143	3.525	-11.396	-4.5885	3.4558

The denormalized input value, X_{in} after the trained network is given by,

$$X_{in} = \frac{(O_{1\,ij} + 1) \times (X_{max} - X_{min})}{2} + X_{min} \quad (18)$$

where X_{max} is the maximum value of the target = 391, X_{min} is the minimum value of the target = 267, X_{in} was determined in terms of $O_{1\,ij}$.

$$X_{in} = \frac{(O_{1\,ij} + 1) \times (391 - 267)}{2} + 267 \quad (19)$$

$$X_{in} = 62(O_{1\,ij} + 1) + 267 \quad (20)$$

The weights and bias generated at the output layer in Table 3 were inserted into equation (12) to obtain $O_{1\,ij}$ on which the Purelin transfer function operated to have N – the normalized predicted output. Denormalizing N and inserting $O_{1\,ij}$ in equation (13) produced equation (21),

$$N = 62 \left[\sum_{i=1,2}^{j=1\ldots5} (WO_{ij} \times F_{ij}) + b_o \right] + 267 \quad (21)$$

where bo is the bias in the output layer, *n* is the sum of the inputs, Wo is the weight in the output layer, (LW) and *j* is the neuron in the output layer. From Table 3, the weights are: [-8.5856, -0.255, -0.821, 0.368, -4.588] and bias (bo = 3.4558] at the output layer. Equation (21) is simplifies to equation (22) when weights are inserted

$$N = 62[W_1F_1 + W_2F_2 + W_3F_3 + W_4F_4 + W_5F_5 + b_o] + 267 \quad (22)$$

$$N = 62 \,[-8.5856F_1 + 0.255F_2 - 0.821 + 0.368F_4 - 4.588F_5 + 3.4558] + 267 \quad (23)$$

$$\therefore N = -532F_1 + 15.81F_2 - 50.9F_3 + 22.82F_4 - 284F_5 + 481.26 \quad (24)$$

These coefficients demonstrate that all of the parameters have a strong relationship with the refractivity, particularly the Temperature and relative humidity. The results further indicate that the relative humidity has greater effects on the refractivity than the other two parameters. Moreover, the relative humidity has a significant influence on the refractivity during the rainy month of August.

4.6   SEASONAL   VARIATION   OF   RADIO REFRACTIVITY

Fig.5 depicts the variations of radio refractivity against the time of the days from January to December 2021. The results obtained shows that, generally, the average radio refractivity shows higher values during the rainy season which could be attributed to high values of relative humidity in the troposphere while the average monthly radio refractivity was low during the dry season which could be attributed to high temperature values and low values of relative humidity. In the environment understudy, the rainy season spans from April to September while dry season spans between October to march. The minimum average radio refractivity value (267 N-units) was obtained in the month of February (dry season) while higher value of 391 N-units was obtained for the month of September (rainy season), this implies that, temperature, relative humidity and atmospheric pressure has direct impact

on radio refractivity. Fig. 6 shows the bar graph of the monthly variation of radio refractivity. From the literature survey, the higher refractivity lowers the signal strength and vice versa (Oluwole and Olayinka 2013). A high refractivity has an effect on the radio signal, and subsequently, the wireless communication system may not function properly. The refractivity is low from January to April, but increases from May to September, and after which declined sharply in October to December. This is due to the fact that the high refractivity can be expected in the rainy season because the relative humidity is high.

The comparison between the ANN predicted refractivity and target refractivity is also presented in Fig.5. The ANN predicted and original values (target) for radio refractivity agree well with each other having the mean square error, MSE = 0.082. Next, the validation between the actual and predicted refractivity shows an error less than 0.5%, which guarantees the accuracy of the suggested ANN. The bar graph shown in Fig.6 revealed the monthly variations of radio refractivity, with the lowest value of N in the dry season (February) while the highest value was obtained in the wet particulate (September)
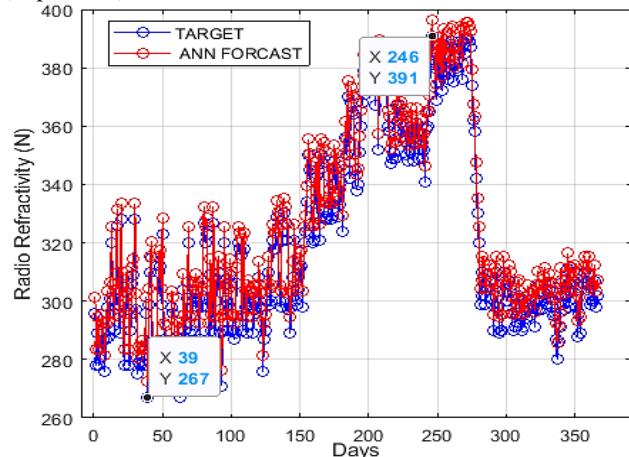

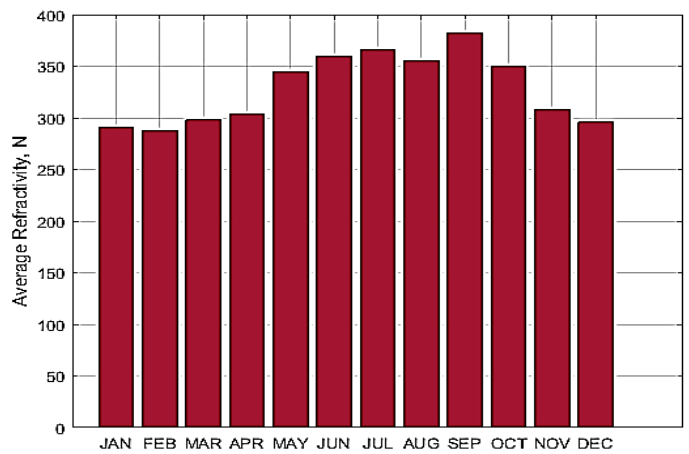**Fig.5 Actual and predicted radio refractivity.**

Fig.6 Monthly variations of radio refractivity

The deviations between the target and ANN forecast were computed using equation(25) and were used in deviation analysis of the developed ANN best model to appraise its accuracy.

$$\text{Margin of deviation} = \left(\frac{N_m - N_c}{N_m}\right) \times 100 \qquad (25)$$

where N_m is the measured radio refractivity and N_c is the

Input	1	2	3	4	5	Sum	impact	Rank
X1	61.0	-3.16	0.95	-6.79	-19.22	32.85	23.92%	2
X2	121.4	-1.44	1.19	4.59	-37.36	88.38	64.37%	1
X3	33.1	0.59	0.01	-1.47	-16.17	16.08	11.71%	3
Sum	215.5	-4.01	2.15	-3.67	-72.75	**137.3**	100%	

ANN computed radio refractivity.

From the visual comparison between the target and the predicted data using the proposed ANN prediction model, the predicted performance data is in good agreement with the experimental data having correlation coefficient 0.917. As depicts inFig.7, the deviation distribution is concentrated around 0 with deviation margin < 0.5% which connotes the high accuracy of the proposed ANN model
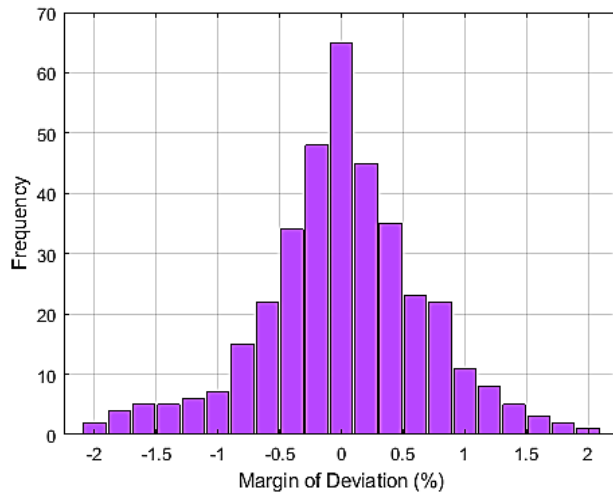

Fig.7 Margin of deviation for ANN predicted radio refractivity

The correlation coefficients of the radio refractivity with the considered meteorological parameters, temperature, relative humidity and pressure, in Ibadan are 0.64, 0.92, and 0.47 respectively. These coefficients establish that all of the parameters have a strong influence with the radio refractivity, particularly the relative humidity and temperature. The results further indicate that the relative humidity has greater effects on the refractivity than the other two parameters The correlation is further justified by determine the relative importance of input parameters using the expression shown in (16) where W_{yz} is the weights from hidden neurons to

output neuron, z is the output neuron (1) and y is the total number of hidden neurons 1, 2, 3, 4 and 5 as presented in Table 4.

4.7 RELATIVE IMPORTANCE OF INPUT PARAMETERS

As presented in Fig.8, relative humidity has the positive and greatest impact with highest rank (64.37%) on radio refractivity. Temperature also have positive effect on refractivity (23.92%) while atmospheric pressure gave least influence on radio refractivity (11.71%). This implies that, increase in temperature, relative humidity and atmospheric pressure leads to increase in radio refractivity.

The ranking is as shown in Table 4.

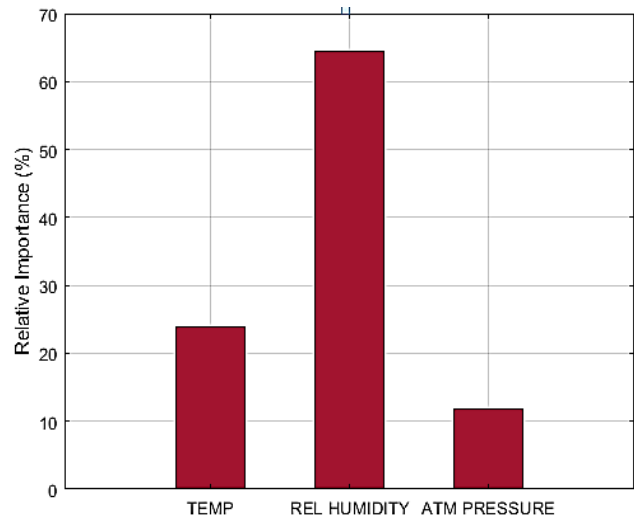Table 4. Relative contribution of each input parameters.

Fig.8 Relative importance of input parameters in ANN model

5. CONCLUSION

In this study, three meteorological parameters namely: temperature, relative humidity and atmospheric pressure were used as inputs in the development of ANN based model for the determination of radio refractivity in Ibadan, South western, Nigeria. The study revealed that, the diurnal and monthly variations of radio refractivity are influenced by three atmospheric parameters namely; Temperature, relative humidity and atmospheric pressure. It was noted that, relative humidity has the greatest influence on refractivity variations followed by temperature. The results further revealed that, the refractivity values are higher during the rainy season owing to a strong association with the temperature and relative humidity, while it was lower in the dry season due to decrease

in values of relative humidity and increase in air temperature. The minimum average radio refractivity value (365.2 N-units) was observed in the month of February (dry season) while higher value of 383 N-units was obtained for the month of September (rainy season). Therefore, it is important to properly cater for the signal communication system during hot and humid weather. Furthermore, the developed model has an acceptable accuracy value as demonstrated from comparison of the ANN predicted with actual measured values having the lowest MSE = 0.082. Based on the results obtained, the proposed ANN technique can be used to develop a refractivity database which is highly important in a radio communication system.

References

Adeniran A.O, Olabisi O, and Ajao O.S (2020). "Spatial coverage of FM radio signal variation measurement and comparison of two major radio stations within AkwaIbom state, 3(3); 1-7.

Aremu, O.A., Olayiwola, O.G., Mufutau, J.A., Anie, N. O. (2021). "Impacts of Refracivity Gradient and Effective Earth's Radius Factor on Radio Signal Propagation at 100 m under clear air in Ibadan South Western Nigeria," *European Modern Study Jouranl*, vol. 5 (3), pp 282-290..

Babin, S.M (1995). "A case study of sub-refractive conditions at Wallops Island, Virginia," *Journal of Applied Meteorology*, vol. 34, pp. 1028-1038.

Bean, B.R., Thayer, G.D (1959). "Models of the atmospheric radio refractive index" *Proceedings of the IRE*, pp. 740-755

Falodun S.E., Ajewole M.O. (2006) Radio refractive index in the lowest 100 m layer of the troposphere in Akure South Western Nigeria. Journal of Atmospheric and Solar-Terrestrial Physics. 2006; 68 (2):236-243.

Gao J, Brewster K, and Xue M. (2008). Variation of radio refractivity with respect to moisture and temperature and influence on radar ray path. *Advances in Atmospheric Sciences*. 2008; 25 (6): 1098±1106.

Google Maps, (2020). Map of UFRN campus. [online]. Google. Available from: https://goo.gl/maps/1RbPQwn5o6y [Accessed 24 November 2020].

Grabner, M. and V. Kvicera, (2003) "Clear-air propagation modeling using parabolic equation method," Radio Engineering, Vol. 12, No. 4, 50–54, 2003.

ITU – R., (2012). The refractive index: its formula and refractivity data, Recommendation 203/1, ITU-R, Pp 453-9.

Olden, J.D., Joy, M.K., Death, R.G., (2004). An accurate comparison of Methods for Quantifying Variable importance in artificial Neural Networks using simulated data. Ecol. Model 178, 389 – 397.

Oluwole F.J, Olayinka O. M. (2013). A test of the relationship between refractivity and radio signal propagation for dry particulates. Research Desk, 2013; 2(4):334–338.

Tohidi, M., Sadeghi, M., Mousavi, S. R., and Mireei, S. A. (2012). Artificial neural network modeling of process and product indices in deep bed drying of rough rice. *Turkish Journal of Agriculture and Forestry*, 36(6), 738-748.

Valma E, Tamosaiunaite M, Tamosaiunas S, Tamosaiuniene M, Zilinskas M. (2015) Determination of radio refractive index using meteorological data. Elektronikair Elektrotechnika. 2015; 106 (10):125-128.